

\mathcal{PT} restoration via increased loss-gain in \mathcal{PT} -symmetric Aubry-Andre model

Charles Liang, Derek D. Scott, and Yogesh N. Joglekar

Department of Physics, Indiana University Purdue University Indianapolis (IUPUI), Indianapolis, Indiana 46202, USA

(Dated: November 12, 2018)

In systems with “balanced loss and gain”, the \mathcal{PT} -symmetry is broken by increasing the non-hermiticity or the loss-gain strength. We show that finite lattices with oscillatory, \mathcal{PT} -symmetric potentials exhibit a new class of \mathcal{PT} -symmetry breaking and restoration. We obtain the \mathcal{PT} phase diagram as a function of potential periodicity, which also controls the location complex eigenvalues in the lattice spectrum. We show that the sum of \mathcal{PT} -potentials with nearby periodicities leads to \mathcal{PT} -symmetry restoration, where the system goes from a \mathcal{PT} -broken state to a \mathcal{PT} -symmetric state as the average loss-gain strength is increased. We discuss the implications of this novel transition for the propagation of a light in an array of coupled waveguides.

Introduction. Open systems with balanced loss and gain have gained tremendous interest in the past three years since their experimental realizations in optical [1–4], electrical [5], and mechanical [6] systems. Such systems are described by non-hermitian Hamiltonians that are invariant under combined parity and time-reversal (\mathcal{PT}) operations [7]. Apart from their mathematical appeal, such non-hermitian Hamiltonians show non-intuitive properties such as unidirectional invisibility [4, 8, 9] and are thus of potential technological importance.

Historically, \mathcal{PT} Hamiltonians on an infinite line were the first to be investigated [10, 11]. The range of parameters where the spectrum of the Hamiltonian is purely real, $\epsilon_\lambda = \epsilon_\lambda^*$, and the eigenfunctions are simultaneous eigenfunctions of the \mathcal{PT} operator, $\psi_\lambda(x) = \psi_\lambda^*(-x)$, is called the \mathcal{PT} -symmetric phase. The emergence of complex conjugate eigenvalues when the parameters are not in this region is called \mathcal{PT} -symmetry breaking. A positive threshold for \mathcal{PT} -symmetry breaking implies that the system transitions [2–6] from a quasi-equilibrium state at a small but nonzero non-hermiticity, to loss of reciprocity as the strength of the balanced loss-gain term crosses the threshold. Although \mathcal{PT} -symmetric Hamiltonian studies started with continuum Hamiltonians, all of their realizations are in finite lattices where the continuum, effective-mass approximation may not apply. This observation has led to tremendous interest in \mathcal{PT} -symmetric lattice models [12–18] that can be realized in coupled waveguide arrays [19, 20].

A universal feature of all such systems is that \mathcal{PT} -symmetry is broken by increasing the balanced loss-gain strength and restored by reducing it. Here, we present a tight-binding model that can exhibit exactly opposite behavior, via a family of \mathcal{PT} -symmetric, periodic potentials.

A remarkable property of lattice models, absent in the continuum limit, is the effects of a periodic potential. The spectrum of a charged particle in constant magnetic field in two dimensions consists of Landau levels [21–23]; a similar particle on a two-dimensional lattice displays a fractal, Hofstadter butterfly spectrum [24–27]. In one dimensional lattices, a fractal spectrum

emerges in the presence of a hermitian, periodic potential, and this model, known as the Aubry-Andre model [28], shows localization transition in a clean system when the strength of the incommensurate potential exceeds the nearest-neighbor hopping [29]. Here, we consider a \mathcal{PT} -symmetric Aubry-Andre model on an N -site lattice with hopping J and complex potential $V_\beta(n) = V_0 \cos[2\pi\beta(n - n_c)] + i\gamma \sin[2\pi\beta(n - n_c)]$ where $n_c = (N + 1)/2$ is the lattice center and $\gamma > 0$. Since $V_\beta = (-1)^{2n_c} V_{1-\beta}^* = (-1)^{2n_c} V_{1+\beta}$, it is sufficient to consider the family of potentials with $0 < \beta < 1$ (when $\beta = 0$ the problem reduces to the Aubrey-Andre model [24, 28]). We then consider the effect of two such potentials $V_{\beta_1} + V_{\beta_2}$ with $|\beta_1 - \beta_2| \sim 1/N \ll 1$.

Our salient results are follows: i) For a single potential V_β , the threshold loss-gain strength $\gamma_{PT}(N, V_0, \beta)$ shows N local maxima along the β axis; it is suppressed by a nonzero real modulation V_0 . ii) The discrete index of pair of eigenvalues that become complex can be tuned stepwise by varying $0 < \beta < 1/2$. iii) For $V = V_{\beta_1} + V_{\beta_2}$, generically, the phase diagram in the (γ_1, γ_2) plane shows a re-entrant \mathcal{PT} -symmetric phase: a broken \mathcal{PT} -symmetry is restored by increasing the non-hermiticity and broken again when γ_i become sufficiently large. This behavior is absent in the extensively studied continuum Hamiltonians with complex potentials [30–32], and is a result of competition between the two lattice potentials V_{β_1} and V_{β_2} .

We emphasize that $\gamma_i > 0$ means the gain-regions of the two potentials mostly align as do their respective loss-regions. Thus, the competition between V_{β_1} and $V_{\beta_2 \approx \beta_1}$ is not in their loss-gain profiles, but, as we will show below, due to the relative locations of \mathcal{PT} -symmetry breaking energy-levels in the spectrum.

\mathcal{PT} phase diagram for a single potential. The tight-binding hopping Hamiltonian for an N -site lattice with open boundary conditions is $H_0 = -J \sum_{n=1}^{N-1} (|n\rangle\langle n+1| + |n+1\rangle\langle n|)$. Its particle-hole symmetric energy spectrum is given by $\epsilon_{0,p} = -2J \cos(k_p) = -\epsilon_{0,\bar{p}}$ and the corresponding normalized eigenfunctions are $\psi_p(j) = \sin(k_p j) = (-1)^j \sin(k_{\bar{p}} j)$ where $0 < k_p = p\pi/(N+1) < \pi$ and $\bar{p} = N + 1 - p$. The properties that relate eigenval-

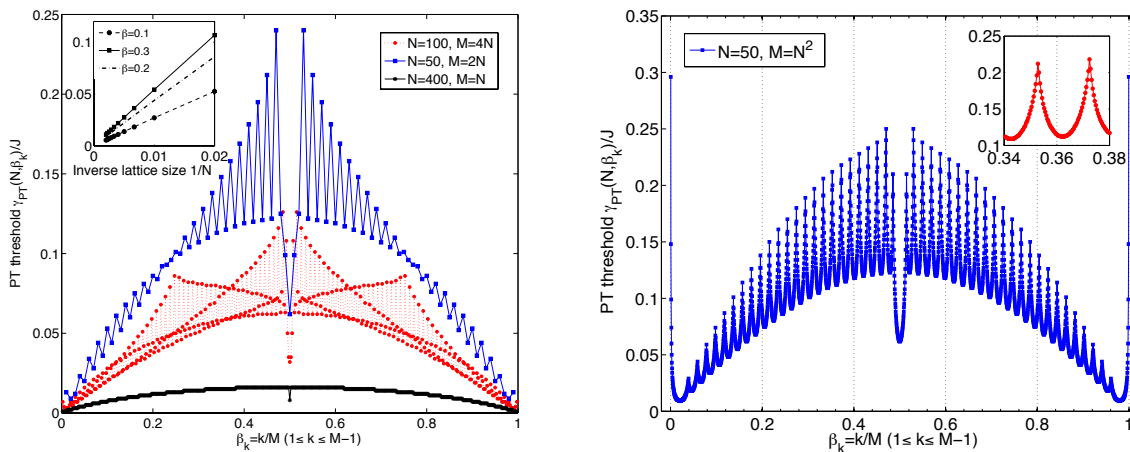


FIG. 1. (color online) Left-hand panel: \mathcal{PT} -symmetric threshold $\gamma_{PT}(N, \beta)$ for $N = 50$ lattice with discretization $\beta_k = k\delta\beta = k/2N$ (blue squares), $N = 100$ lattice with $\delta\beta = 1/4N$ (red markers), and $N = 400$ lattice with $\delta\beta = 1/N$ (black stars) shows that the phase-diagram depends sensitively on $\delta\beta \sim O(1/N)$. The inset shows that for a fixed β , the threshold is linearly suppressed, $\gamma_{PT}(N, \beta) = C_\beta/N$. Right-hand panel: Results are independent of the discretization when $\delta\beta \sim 1/N^2 \ll 1/N$ and the $N = 50$ phase-diagram shows N local maxima and smooth oscillations with period $\Delta\beta = 1/N$ (inset).

ues and eigenfunctions at indices p, \bar{p} remain valid in the presence of pure loss-gain potential $V_\beta = -V_\beta^*$ [33]. The eigenvalue equation for an eigenfunction $f(n)$ of the non-Hermitian, \mathcal{PT} -symmetric Hamiltonian $H_\beta = H_0 + V_\beta$ is given by ($1 \leq n \leq N$)

$$-J[f(n+1) + f(n-1)] + V_\beta(n)f(n) = Ef(n), \quad (1)$$

with $f(0) = 0 = f(N+1)$. Since this difference equation is not analytically soluble for an arbitrary β , we numerically obtain the spectrum $E(\gamma)$ and the \mathcal{PT} -symmetry breaking threshold $\gamma_{PT}(N, V_0, \beta)$ using different discretizations $\beta_k = k\delta\beta$ along the β -axis. Due to the $\beta \leftrightarrow 1 - \beta$ symmetry of the potential, it follows that the exact threshold loss-gain strength satisfies $\gamma_{PT}(N, V_0, \beta) = \gamma_{PT}(N, V_0, 1 - \beta) = \gamma_{PT}(N, -V_0, \beta)$.

We consider a purely loss-gain potential, present results for an even lattice, and point out the salient differences that arise when lattice size N is odd or when $V_0 \neq 0$. The left-hand panel in Fig. 1 shows the \mathcal{PT} -symmetric threshold $\gamma_{PT}(N, \beta)/J$ for an $N = 50$ lattice obtained by using discretization $\delta\beta = 1/2N$ (blue squares), an $N = 100$ lattice with $\delta\beta = 1/4N$ (red markers), and an $N = 400$ lattice with $\delta\beta = 1/N$ (black stars). There is a monotonic suppression of the threshold strength with increasing N , and, crucially, the general shape of the phase diagram depends upon the size of $\delta\beta$ relative to $1/N$. A scaling of this threshold suppression for lattice sizes $N = 50 - 500$, shown in the inset, implies that $\gamma_{PT}(N, \beta) = C_\beta/N$ where C_β is a constant. Thus, the threshold strength is suppressed linearly and vanishes in the thermodynamic limit [34, 35]. However, this algebraically fragile nature of the \mathcal{PT} -phase is not an impediment since \mathcal{PT} -systems to-date are only realized

in small lattices with $N \ll 100$. The right-hand panel in Fig. 1 shows the phase diagram for $N = 50$ case with discretization $\delta\beta = 1/N^2$. The results for irrational values of β and other discretizations lie on the same curve. The \mathcal{PT} phase diagram shows $(N - 2)$ local maxima located at $\beta_k = (2k + 1)/2N$ and the two maxima at the end points, is symmetric about the center and has a local minimum in the threshold at $\beta = 1/2$. In addition, the function $\gamma_{PT}(N, \beta)$ has $(N - 1)$ minima at $\beta_k = k/N$ and smoothly oscillates over a period $\sim 1/N = 0.02$ as shown in the inset (solid red circles). These results are generic for any lattice size N with discretization $\delta\beta \sim 1/N^2$.

When N is odd, the non-Hermitian potential vanishes at $\beta = 1/2$ and the spectrum of the Hamiltonian H_β is purely real. For an odd lattice, a similarly obtained phase diagram shows $(N - 1)$ local maxima that are distributed equally on the two sides of $\beta = 1/2$, along with a substantial enhancement in the threshold strength as $\beta \rightarrow 1/2^\pm$. Adding a real potential modulation $V_0 \neq 0$, to the loss-gain potential, in general, suppresses the threshold strength.

The phase diagram can be understood as follows: for a small $\beta \sim 1/N^2 \ll 1/N$, $V_\beta(n) = i\gamma(2\pi\beta)(n - n_c)$ and the enhanced \mathcal{PT} -breaking threshold, $\gamma_{PT}/J \sim 0.3$, is consistent with a linear-potential threshold [36]. For an even lattice, the average of the gain-potential is given by $A_E(\beta) = \sum_{n>n_c}^N V_\beta(n)/i\gamma = \sin^2(N\pi\beta/2)/\sin(\pi\beta) \geq 0$. The \mathcal{PT} threshold is greatest when the *change in the average strength is maximum* as β is varied, $\partial_\beta^2 A_E(\beta) = 0$. In the limit $N \gg 1$ and $\beta \gg 1/N^2$, it implies that the N maxima of $\gamma_{PT}(N, \beta)$ occur at $\beta_{k, \max} = (2k + 1)/2N$. On the other hand, $\gamma_{PT}(N, \beta)$ is smallest when the *change in the average strength is minimum*, $\partial_\beta A_E(\beta) = 0$, and gives

the locations of $(N-1)$ minima as $\beta_{k,\min} = k/N$. A similar analysis applies to odd lattices, where the average potential is given by $A_O(\beta) = \sin[\pi\beta(N-1)/2] \sin[\pi\beta(N+1)/2] / \sin(\pi\beta)$.

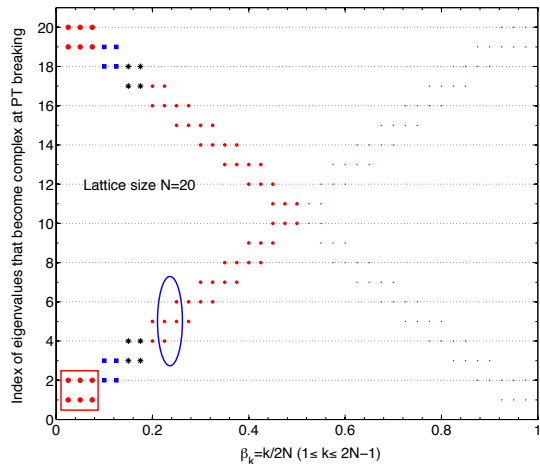


FIG. 2. (color online) Index of eigenvalues that become complex as a function of β for an $N = 20$ lattice with discretization $\delta\beta = 1/2N = 0.025$ shows a $\beta \leftrightarrow 1 - \beta$ symmetry, denoted by heavy and light red markers. When $\beta \leq 0.08$, levels (E_1, E_2) become degenerate and complex, and so do their particle-hole counterparts, (E_{19}, E_{20}) (red circles); in general, we can tune the location of \mathcal{PT} -breaking (blue squares, black stars, red markers) by appropriately choosing β .

Next, we focus on the *location* of the \mathcal{PT} symmetry breaking. Due to the particle-hole symmetric spectrum of H_β , two pairs of levels (E_n, E_{n+1}) and $(-E_n, -E_{n+1})$ become complex simultaneously. Figure 2 plots the indices of eigenvalues that become complex as a function of β for an $N = 20$ lattice with discretization $\delta\beta = 1/2N$. It shows that at small β , the eigenvalues at the band edges become complex, whereas, as $\beta \rightarrow 1/2$, the pairs of eigenvalues that become complex move to the center of the band. Thus the average range of β s with the same location for \mathcal{PT} -symmetry breaking is $\sim 1/N$. It follows that by choosing an appropriate β , one is able to control the location of \mathcal{PT} -symmetry breaking in the energy spectrum. As we will see next, this control allows us to introduce competition between potentials V_β with two different, but close, values of β .

\mathcal{PT} phase diagram with two potentials. We now consider the \mathcal{PT} -symmetric phase of the Hamiltonian with two potentials, $H = H_0 + V_{\beta_1} + V_{\beta_2}$, in the (γ_1, γ_2) plane, where both axes are scaled by their respective threshold values $\gamma_{jPT} = \gamma_{PT}(\beta_j)$. Panel (a) in Fig. 3 shows the numerically obtained phase diagram for an $N = 20$ lattice with $(\beta_1, \beta_2) = (0.20, 0.25)$ (blue stars and squares). It shows that, from a \mathcal{PT} -broken phase (point 1), it is possible to enter the \mathcal{PT} -symmetric phase by increasing the non-hermiticity γ_1 (point 2). We emphasize that increas-

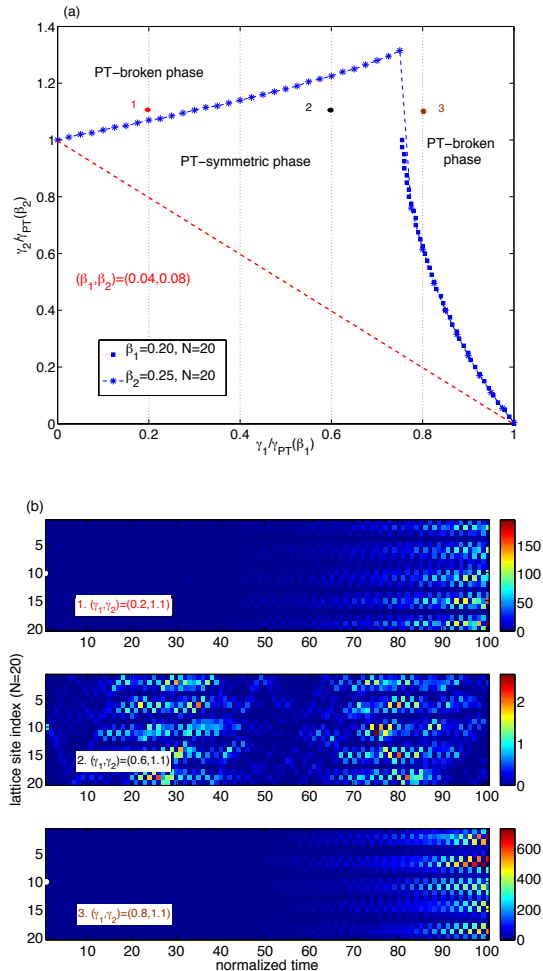


FIG. 3. (color online) Panel (a): \mathcal{PT} -phase diagram for potential $V_{\beta_1} + V_{\beta_2}$. When $(\beta_1, \beta_2) = (0.20, 0.24)$ (blue stars and squares), a \mathcal{PT} -broken phase (point 1) is restored by increasing γ_1 (point 2) and subsequently broken again (point 3). This re-entrant phase is due to competition between V_{β_1} and V_{β_2} . For $(\beta_1, \beta_2) = (0.04, 0.08)$, the two co-operate and the phase boundary is an expected straight line. Panel (b): intensity $I(k, t)$ of an initially normalized state shows that, starting from a \mathcal{PT} -broken phase (top panel), increasing γ_1 initially restores bounded oscillations (center panel), followed by \mathcal{PT} breaking and amplification (bottom panel). Note the two-orders-of-magnitude difference in the total intensity.

ing γ_1 increases the average gain- (and loss-) strength $\gamma_1 A_E(\beta_1) + \gamma_2 A_E(\beta_2)$, and yet drives the system into a \mathcal{PT} -symmetric phase from a \mathcal{PT} -broken phase. Increasing γ_1 further, eventually, drives the system into a \mathcal{PT} broken phase again (point 3).

While a \mathcal{PT} -broken phase implies an exponential time-dependence of the net intensity or the norm of a state, in the \mathcal{PT} -symmetric phase the net intensity oscillates within a bound that is determined by the proximity of the Hamiltonian to the \mathcal{PT} phase boundary [20]. Panel (b) in Fig. 3 shows the dramatic consequences of \mathcal{PT}

restoration on the site- and time-dependent intensity $I(k, t) = |\langle k | \exp(-iHt/\hbar) | \psi_0 \rangle|^2$ of a state $|\psi_0\rangle$ that is initially localized on site $N/2 = 10$; the time is measured in units of \hbar/J . The top-subpanel shows that intensity has a monotonic amplification in regions with gain sites, leading to a striated pattern (point 1). Center subpanel shows that by increasing γ_1 , oscillatory behavior in the intensity is restored (point 2). Bottom subpanel shows that increasing γ_1 further breaks the \mathcal{PT} symmetry again (point 3). Thus, we are able to *restore \mathcal{PT} -symmetry by increasing the non-hermiticity*, and achieve amplification by both reducing or increasing the average gain-strength. This novel behavior is absent in all lattice models with a single \mathcal{PT} potential.

Since each potential V_{β_j} breaks the \mathcal{PT} symmetry for $\gamma_j/\gamma_{jPT} > 1$, naively, one may expect that the \mathcal{PT} phase boundary for $V_{\beta_1} + V_{\beta_2}$ is given by $\gamma_1/\gamma_{1PT} + \gamma_2/\gamma_{2PT} = 1$. This is indeed the case for $(\beta_1, \beta_2) = (0.04, 0.08)$, shown by red dashed line in panel (a), even though the potential periodicities differ by a factor of two.

What is the key difference between the two sets of parameters, one of which shows a re-entrant \mathcal{PT} -symmetric phase? It is the indices of eigenvalues that become complex due to V_{β_1} and V_{β_2} . The red rectangle in Fig. 2 shows that for $\beta \leq 0.8$, eigenvalues (E_1, E_2) become complex. In such a case, the two potentials V_{β_1} and V_{β_2} act in a cooperative manner effectively adding their strengths. Therefore, the \mathcal{PT} -phase boundary is a straight line. In contrast, the blue oval in Fig. 2 shows that for $\beta_1 = 0.20$, energy levels E_4, E_5 approach each other, become degenerate, and then complex as $\gamma \rightarrow \gamma_{1PT}$; for $\beta_2 = 0.25$, the energy levels that become complex as $\gamma \rightarrow \gamma_{2PT}$ are E_5, E_6 . Thus, the level E_5 is *lowered by potential V_{β_1} and raised by the potential V_{β_2}* from its hermitian-limit value. This introduces competition between the two potentials V_{β_1} and V_{β_2} even though their gain-regions largely overlap and so do their respective loss regions.

This correspondence between competing potentials and \mathcal{PT} -restoration is further elucidated in Fig. 4. In conjunction with Fig. 2, it shows that re-entrant \mathcal{PT} -symmetric phase occurs when the two potentials compete (panels b-e, g, h). This restoration of \mathcal{PT} -symmetry can be due to increased loss-gain strength in γ_1 (panels d, e), γ_2 (panels b, c, g), or both (panel h). On the other hand, when the two potentials break the same set of eigenvalues, the \mathcal{PT} phase boundary is a line (panels a, f, k).

Discussion. Competing potentials, a common theme in physics, often stabilize phases that would be unstable in the presence of only one of them [37]. A trivial definition of competing \mathcal{PT} -potentials is that the gain-region of one strongly overlaps with the loss-region of another, thus reducing the average gain (and loss) strength.

Here, we have unmasked the subtle competition between \mathcal{PT} potentials whose gain regions largely overlap, based on the location of \mathcal{PT} -symmetry breaking induced by each. This competition results in \mathcal{PT} -restoration and

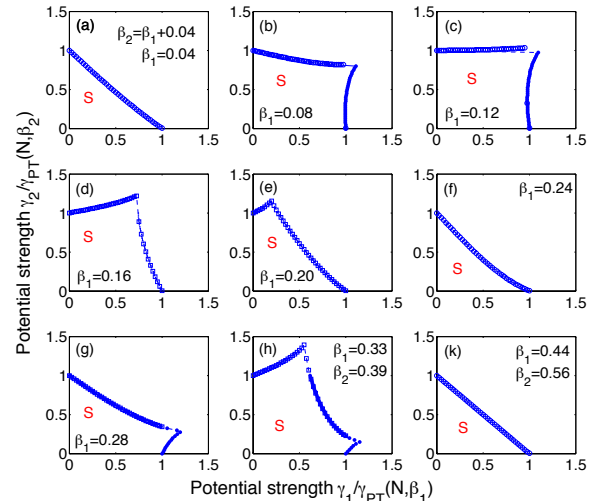


FIG. 4. (color online) \mathcal{PT} -phase boundary for an $N = 20$ lattice with potentials $V_{\beta_1} + V_{\beta_2}$ shows that \mathcal{PT} -symmetry restoration can occur by increasing non-hermiticity γ_1 (panels b, c, g), γ_2 (panels d, e), or both (panel h) when the two potentials compete. When they make complex the same set of eigenvalues, the phase boundary is a line (panels a, f, k). The label “S” denotes the \mathcal{PT} -symmetric phase.

subsequent \mathcal{PT} -breaking, leading to selective intensity suppression and oscillations at large loss-gain strength. Its hints were seen in a continuum model with complex δ -function and constant potentials, but that continuum model is neither easily experimentally realizable nor can it tune between cooperative and competitive behavior [39]. The \mathcal{PT} -symmetric Aubry-Andre model provides a family of potentials with tunable competition or cooperation among them, and is thus ideal for investigating the consequences of such competition; even lattices as small as $N = 10$ that can be realized via coupled optical waveguides [19, 20] or cold atoms [38] may provide a comprehensive understanding of interplay between loss-gain strengths and \mathcal{PT} -symmetry breaking.

This work was supported by NSF Grant No. DMR-1054020.

-
- [1] A. Guo, G.J. Salamo, D. Duchesne, R. Morandotti, M. Volatier-Ravat, V. Aimez, G.A. Siviloglou, and D.N. Christodoulides, Phys. Rev. Lett. **103**, 093902 (2009).
 - [2] C.E. Rüter, K.G. Makris, R. El-Ganainy, D.N. Christodoulides, M. Segev, and D. Kip, Nat. Phys. **6**, 192 (2010).
 - [3] L. Feng, M. Ayache, J. Huang, Y.-L. Xu, M.-H. Lu, Y.-F. Chen, Y. Fainman, and A. Scherer, Science **333**, 729 (2011).
 - [4] A. Regensburger, C. Bersch, M.-A. Miri, G. Onishchukov, D.N. Christodoulides, and U. Peschel, Nature **488**, 167 (2012).

- [5] J. Schindler, A. Li, M.C. Zheng, F.M. Ellis, and T. Kottos, *Phys. Rev. A* **84**, 040101(R) (2011).
- [6] C.M. Bender, B.K. Berntson, D. Parker, and E. Samuel, *Am. J. Phys.* **81**, 173 (2013).
- [7] For a review, see C.M. Bender, *Rep. Prog. Phys.* **70**, 947 (2007) and references therein.
- [8] Z. Lin, H. Ramezani, T. Eichelkraut, T. Kottos, H. Cao, and D.N. Christodoulides, *Phys. Rev. Lett.* **106**, 213901 (2011).
- [9] L. Feng, Y.-L. Xu, W.S. Fegadolli, M.-H. Lu, J.E.B. Oliveira, V.R. Almeida, Y.-F. Chen, and A. Scherer, *Nat. Mater.* **12**, 108 (2013).
- [10] C.M. Bender and S. Boettcher, *Phys. Rev. Lett.* **80**, 5243 (1998).
- [11] C.M. Bender, D.C. Brody, and H.F. Jones, *Phys. Rev. Lett.* **89**, 270401 (2002).
- [12] M. Znojil, *Phys. Rev. A* **82**, 052113 (2010).
- [13] M. Znojil, *Phys. Lett. A* **375**, 3435 (2011).
- [14] O. Bendix, R. Fleischmann, T. Kottos, and B. Shapiro, *Phys. Rev. Lett.* **103**, 030402 (2009).
- [15] L. Jin and Z. Song, *Phys. Rev. A* **80**, 052107 (2009).
- [16] Y.N. Joglekar and A. Saxena, *Phys. Rev. A* **83**, 050101(R) (2011).
- [17] G. Della Valle and S. Loghi, *Phys. Rev. A* **87**, 022119 (2013).
- [18] S. Longhi, G. Della Valle, *Ann. Phys.* **334**, 35 (2013).
- [19] D.N. Christodoulides, F. Lederer, and Y. Silberberg, *Nature (London)* **424**, 817 (2003).
- [20] Y.N. Joglekar, C. Thompson, D.D. Scott, and G. Vemuri, *Eur. Phys. J. Appl. Phys.* **63**, 30001 (2013).
- [21] See chapter XV, L.D. Landau and E.M. Lifshitz, *Quantum Mechanics (Non-relativistic Theory)* (Butterworth-Heinemann, Burlington, MA, 2005).
- [22] F.D.M. Haldane, *Phys. Rev. Lett.* **61**, 2015 (1988).
- [23] Y. Zheng and T. Ando, *Phys. Rev. B* **65**, 245420 (2002).
- [24] P. Harper, *Proc. Phys. Soc. London Sec. A* **68**, 874 (1955).
- [25] D. Hofstadter, *Phys. Rev. B* **14**, 2239 (1976).
- [26] M. Aidelsburger, M. Atala, M. Lohse, J. T. Barreiro, P. Paredes, and I. Bloch, *Phys. Rev. Lett.* **111**, 185301 (2013); H. Miyake, G.A. Siviloglou, C.J. Kennedy, W.C. Burton, and W. Ketterle, *ibid* 185302 (2013).
- [27] L.A. Ponomarenko *et al.*, *Nature (London)* **497**, 594 (2013); C.R. Dean *et al.*, *ibid* 598 (2013).
- [28] S. Aubry and G. Andre, *Ann. Isr. Phys. Soc.* **3**, 133 (1980).
- [29] Y. Lahini, R. Pugatch, F. Pozzi, M. Sorel, R. Morandotti, N. Davidson, and Y. Silberberg, *Phys. Rev. Lett.* **103**, 013901 (2009).
- [30] K.G. Makris, R. El-Ganainy, D.N. Christodoulides, Z.H. Musslimani, *Phys. Rev. Lett.* **100**, 103904 (2008).
- [31] S. Longhi, *Phys. Rev. A* **81**, 022102 (2010).
- [32] E.-M. Graefe and H.F. Jones, *Phys. Rev. A* **84**, 013818 (2011).
- [33] Y.N. Joglekar, *Phys. Rev. A* **82**, 044101 (2010).
- [34] Y.N. Joglekar, D. Scott, M. Babbey, and A. Saxena, *Phys. Rev. A* **82**, 030103(R) (2010).
- [35] D.E. Pelinovsky, P.G. Kevrekidis, and D.J. Frantzeskakis, *EPL* **101**, 11002 (2013).
- [36] M. Serbyn, M.A. Skvortsov, *Phys. Rev. B* **87**, 020501 (2013).
- [37] See, for example, E. Fradkin, *Field Theories of Condensed Matter Systems* (Addison Wesley, Reading, MA, 1991).
- [38] H. Li, J. Dou, and G. Huang, *Opt. Express* **21**, 32053 (2013).
- [39] Y.N. Joglekar and B. Bagchi, *J. Phys. A* **45**, 402001 (2012).